Electrochemical Impedance Sensing of DNA Hybridization on Conducting Polymer Film-Modified Diamond

Huiru Gu,[†,‡] Xiao di Su,[*,†] and Kian Ping Loh[*,‡]

Institute of Materials Research and Engineering, 3 Research Link, Singapore 117602, and Department of Chemistry, National University of Singapore, 3 Science Drive 3, Singapore 117543

Received: February 4, 2005; In Final Form: April 11, 2005

The impedimetric sensing of DNA hybridization on polyaniline/polyacrylate (PANI/PAA)-modified boron-doped diamond (BDD) electrode has been investigated. An ultrathin film of PANI−PAA copolymer was electropolymerized onto the diamond surfaces to provide carboxylic groups for tethering to DNA sensing probes. The electrochemical impedance and the intrinsic electroactivity of the polymer-diamond interface were analyzed after the hybridization reaction with target and non-target DNA. The impedance measurement shows changes in the impedance modulus as well as electron-transfer resistance at the stage of probe DNA immobilization (single-strand), as well as after hybridization with target DNA (double-strand). DNA hybridization increases the capacitance of the polymer−DNA layer and reduces the overall impedance of the DNA−polymer−diamond stack significantly. The polymer-modified BDD electrode shows no detectable nonspecific adsorption, with good selectivity between the complementary DNA targets and the one-base mismatch targets. The detection limit was measured to be 2×10^{-8} M at 1000 Hz. Denaturing test on the hybridized probe and subsequent reuse of the probe indicates chemical robustness of the sensor. Our results suggest that electropolymerization followed by the immobilization of biomolecules is a simple and effective way of creating a functional biomolecular scaffold on the diamond surface. In addition, label-free electrochemical impedance method can provide direct and noninvasive sensing of DNA hybridization on BDD.

1. Introduction

Electrochemical impedance (EIS) is a useful tool for analyzing the changes in interfacial properties of modified electrodes (or semiconductor) induced by binding of charged biomolecules on the surfaces. The advantages of EIS include the noninvasive method of detection as compared to voltammetric methods; the application of an oxidative potential in the latter method inevitably results in the irreversible oxidation of the biomolecules. Another practical consideration is the fact that voltammetric measurement is often inhibited by the highly insulating nature of the biomolecular scaffolding on the electrode surface, whereas impedimetric measurements works well even on insulating substrates. To date, the successful applications of impedance spectroscopy have been reported for immunosensors,[1,2] enzyme sensors,[3−5] and DNA sensors.[6−13] Both Faradic and non-Faradic impedance spectroscopy have been applied for the studies of DNA hybridization, either by studying the diffusion of redox probes in the buffer solution[6,9] or by recording the impedance changes of DNA layers[10,11] before and after hybridization. If a semiconductor is used as the signal transducer, a field effect could be induced by the binding of the negatively charged DNA, resulting in distinct changes in the interfacial impedance at certain measuring frequencies.[12,13]

Boron-doped diamond (BDD) is expected to be the next generation of electrode materials because of its attractive electrochemical features, which include a wide electrochemical potential window in aqueous and nonaqueous media, a very low double-layer capacitance, extreme electrochemical stability, and high resistance to fouling and insensitivity to dissolved oxygen.[14−17] Yang and co-workers[13] immobilized DNA on covalently functionalized nanocrystalline and studied in detail the impedance change induced by DNA hybridization. Their modification method is based on photochemically linking the diamond surface with 10 aminodec-1-ene, which were then subsequently linked to thiol-functionalized DNA molecules via a cross linker. Several wet chemical processing steps were involved in such a method. In this study, we used a simple one-step electropolymerization method to introduce a self-terminating ultrathin layer of polyaniline (PANI)/poly(acrylic acid) (PAA) copolymer film on the boron-doped diamond (BDD) surface. The ultrathin polymer matrix has a high density of carboxylic functionalities for tethering to DNA probes with the alkylamino modifier at the 5′ end. Diamond sensors fabricated by such method show good stability and sensitivity comparable with that reported on carbon nanotubes.[11]

2. Experimental Section

Chemical Reagents. Phosphate buffer solution (PBS, pH 7.4) was obtained by dissolving one tablet of the solid phosphate (Sigma) in 200 mL of deionized water (18.2 MΩ cm). *N*-Ethyl-*N*′-[3-(dimethylamino)propyl] (EDC), poly(acrylic acid) (MW = 2000), and aniline monomer were purchased from Sigma and used directly without further purification. The 30 mer oligonucleotides were synthesized by MWG Biotech. The probe DNA is modified at the 5′ end with an alkylamino modifier (NH_2-ssDNA probes, sequence: NH_2-C_{12}-5′-GCA CCT GAC TCC

* Corresponding author. E-mail: chmlohkp@nus.edu.sg (K. P. Loh); xd-su@imre.a-star.edu.sg (X.d.S.).
† Institute of Materials Research and Engineering.
‡ National University of Singapore.

10.1021/jp050625p CCC: $30.25
Published on Web 06/28/2005

TGT GGA GAA GTC TGC CGT-3′) for immobilization. The target DNAs contain either fully complementary sequence to the probe DNA (5′-ACG GCA GAC TTC TCC ACA GGA GTC AGG TGC-3′) or one-base mismatch to the probe DNA (5′-ACG GCA GAA TTC TCC ACA GGA GTC AGG TGC-3′). The complementary targets for stability test under the fluorescence microscopy detection were labeled by FITC at 3′ end. 0.1 M Na_3PO_4 buffer solution (pH 7.0) and 2×SSC buffer (pH 7.0, containing 0.3 M NaCl and 0.03 M sodium citrate) were used for probe DNA immobilization and target hybridization, respectively.

Preparation of BDD Substrates. 50 μm-thick BDD films were grown on p-doped Si substrates in a commercial 2.45 GHz microwave plasma reactor (Astex) using methanol and boron oxide mixtures, following the established procedure.[18] The BDD diamond has a resistivity of 10 Ω cm, and the boron doping level is approximately 10^{20} cm^{-3}. The films consist of 200 nm sized sharply faceted crystals with roughness of about 60 nm (data from AFM). The resulting substrates were cut into 5 × 5 mm^2 square and used as working electrodes.

Electrogeneration of Polyaniline (PANI)/Poly(acrylic acid) (PAA) Polymer Composite Films and Characterization. Polyaniline (PANI)/poly(acrylic acid) (PAA) films were polymerized on the BDD working electrodes in a 0.1 M H_2SO_4/0.5 M Na_2SO_4 solution containing a 0.2 M aniline monomer and 25 mg/mL poly (acrylic acid) by potential cycling one time from −0.2 to +1.2 V (vs Ag/AgCl) at scan rates of 10 mV/s (or at scan rates of 30, 50, 70, 100 mV/s, respectively, according to experiment needs). The resulting BDD electrodes surfaces were rinsed thoroughly by 0.1 M H_2SO_4/0.5 M Na_2SO_4 electrolyte, deionized water, and dried by a N_2 flow.

An X-ray photoelectronic spectroscopy (XPS, VG ESCALAB 220i-XL Instrument) equipped with an unmonochromated Mg Kα X-ray source (1253.6 eV photons) was used for the analysis of the surface composition of the polymer films. A surface profiler (KLA-TENCHOR Corp. P-10 surface profiler) and a scanning electron microscope (SEM, JEOL JSM-5600LV) were used for quantification of the film thickness and for analysis of the surface morphology of the PANI/PAA polymer composite films.

The carboxyl group density of the copolymer films was quantified using the Toluidine Blue O (TBO) method.[19] In brief, the polymer-modified BDD samples were soaked in an aqueous solution of 5 × 10^{-4} M TBO, adjusted to pH 10 with NaOH. The formation of ionic complexes between the carboxyl groups of the PANI/PAA polymer composite film and the cationic dye was allowed to proceed for 5 h at room temperature, followed by rinsing the samples with a NaOH solution (pH 10) to remove the uncomplexed TBO molecules. Desorption of the dye was performed in 50 wt % acetic acid solution. The amount of the carboxyl groups was calculated from the optical density of the desorbed dye at 633 nm, with the assumption that 1 mol of TBO had complexed with 1 mol of carboxyl groups of the PAA polymer.[19]

DNA Probes Immobilization and Targets Hybridization. For the immobilization of the probe DNA (NH_2-ssDNA), the PANI/PAA-modified BDD electrodes were dipped into a mixture of the NH_2-ssDNA (2 μM in 0.1 M Na_3PO_4 buffer) solution with 20 mg/mL of *N*-ethyl-*N*′-[3-(dimethylamino)-propyl] (EDC) and put in a humidity controlled container for incubation for 10 h. At the end of the incubation, the BDD electrodes were rinsed thoroughly with the immobilization buffer (0.1 M Na_3PO_4) and exposed to 25 μL of the ssDNA targets (either the fully complementary target or the target with one-base mismatch, in 2×SSC buffer) for hybridization. After 30 min, the BDD electrodes were rinsed with the hybridization buffer (2×SSC). The fluorescein (FITC) labeled complementary DNA targets were assayed by a fluorescence microscope (Nikon ECLIPSE, E600).

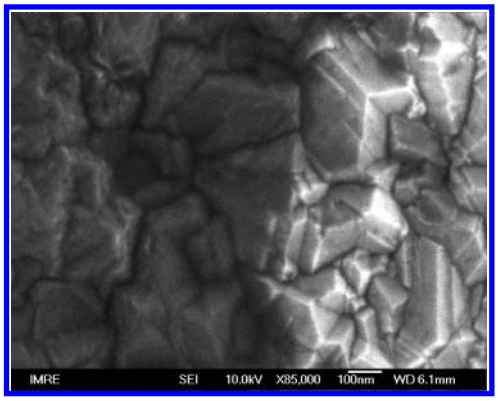

Figure 1. SEM image of PANI/PAA-modified BDD electrode surface (left part: dark) and naked BDD electrode (right part: light).

Stability Test of the PANI/PAA- and DNA/PANI/PAA-Modified BDD. To test the stability of the polymer- and DNA/polymer-modified BDD, denaturing experiments were conducted in four different types of reagents, including 0.05 M NaOH, 0.05 M HCl, 0.1% SDS solution, and hot water (T > melting temperature of the double-helix DNA), to allow the immobilized DNA probe for new cycles of hybridization with the FITC-labeled target DNA. After each cycle of denature and rehybridization, the fluorescent images were taken and the fluorescence intensity was recorded.

Electrochemical System. A three-electrode system was used for polymer electrochemical deposition and for EIS measurements. The doped diamond is used as working electrode, and a Ag/AgCl (in saturated KCl) electrode and a Pt wire were used as the reference counter electrodes, respectively. The cyclic voltammetry was recorded by using a potentiostat/galvanostat and a lock-in amplifier (PAR EG&G model 273A).

The impedance spectra for the polymer-modified BDD and DNA-modified BDD were measured with the above-described potentiostat at a given open circuit voltage from 100 kHz down to 0.1 Hz at a sampling rate of 10 points per decade (AC amplitude 10mV). The data analysis was performed by the Gamry Echem Analyst software, and the equivalent circuit modeling was constructed using the graphical Model Editor software.

3. Results and Discussion

Characterization of Polyaniline (PANI)/Poly(acrylic acid) (PAA) Polymer Composite Film-Modified Boron-Doped Diamond Electrode. Figure 1 shows a SEM image of the BDD where one-half has been modified with PANI/PAA (left), while the other half is left intact (right). The preparation of the partially modified surface was achieved by protecting one-half of the BDD with nail polish before the electropolymerization of the PANI/PAA film. It is obvious that the modified side is visibly darker than the naked side. At the modified side, the surface morphology of the BDD electrode underneath the polymer modify layer can still be seen.

Figure 2 shows the surface profiler (stylus) measurements of the thickness of the polymer films deposited at different scan rates. The film thickness decreases with the decrease of the scan rate. Using a lower scan rate, the thickness of the polymer film can be controlled between 20 and 30 nm as measured by a surface profiler. Optimization of the conditions could be

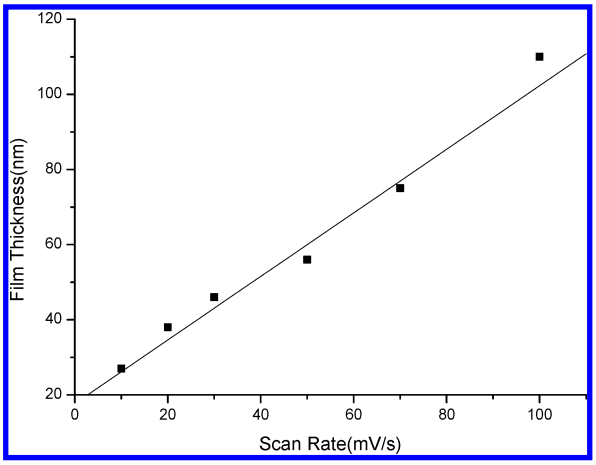

Figure 2. Film thickness of PANI/PAA polymer composite electrochemically deposited on BDD electrode using different scan rates.

achieved at a scan rate of 10 mV/s to attain an ultrathin polymer film with the highest carboxylic functionalities. (COOH group density versus scan rate relationship is shown in Figure 4.)

Figure 3a−d shows the C1s and N1s core-level spectra of the BDD before and after modification with the PANI/PAA polymer composite film. The small but distinct high-BE C1s component at about 288.7 eV in Figure 3c is characteristic of the carboxylic acid group of poly(acrylic acid).[20] The appearance of this component thus indicates clearly the presence of carboxyl groups on the PANI/PAA-modified BDD. The N1s spectra in Figure 3d can be deconvoluted into characteristic components of polyaniline such as quinonoid imine (═N− structure), benzenoid amine (−NH− structure), and positively charged nitrogens with binding energies (BE) at 398.2, 399.4, and 400 eV, respectively.[20−22]

To determine the composition of PANI/PAA polymer composite film on BDD electrodes, the ratio of the peak intensities of the C 1s component at 288.7 eV to that of the total N 1s area, that is, the [COOH]/[N] ratio, was used to quantify the amount of poly(acrylic acid) electrodeposited on the surface. Figure 4 shows the [COOH]/[N] ratio and the density of the carboxyl groups on the PANI/PAA-modified BDD electrodes versus the scan rate of the film. It is found that a lower scan rate produces a higher density of carboxyl groups in the PANI/PAA composite film.

Stability Test of PANI/PAA-Modified BDD and DNA/PANI/PAA-Modified BDD. For the stability test, the PANI/PAA-modified BDD electrodes were first treated with various denature reagents. The resulting films are observed under SEM. Comparing the SEM pictures of the PANI/PAA-modified BDD before and after immersing the samples in four different denature reagents for 2 h, the polymer film on BDD surface appears to be intact. The stability of the immobilized DNA probe was further confirmed by denaturing the DNA duplex using 0.05 M NaOH, and then followed by rehybridization with the FITC-labeled complementary DNA target. Figure 5 shows the FITC intensity of the surface subjected to multiples cycles of denature and re-hybridization. The constant intensity of the fluorescence proves that that the PANI/PAA-modified BDD is very stable and the carboxylic functionality on the surface is not affected after the denature cycles.

Electrochemical Impedance Spectroscopy Study of PANI/PAA-Modified BDD. Impedance spectroscopy allows the detection of capacitance changes at the interfaces during biorecognition events. These capacitance changes can be derived from the imaginary part, Z_{im}, of the complex impedance spectra. The interfacial capacitance can be measured at various biasing potentials (differential capacitance), thus allowing the electrical probing of the system when different charges exist at the electrode. For example, antigens and antibodies are usually charged protein molecules; formation of the bioaffinity complexes between them could be affected by the charge applied onto the electrode surface. Therefore, capacitance changes during the formation of the bioaffinity complexes are potential dependent and the optimal conditions for their measurements could be found. Two convenient ways of treating the impedance data are the Nyquist plot, in which the imaginary number $Z''(\omega)$ are plotted against real number $Z'(\omega)$, and the Bode plot, in which the absolute values of impedance or phase angle are plotted against the frequency. Both types of plots provide information on the nature of electrochemical process occurring at the electrode/electrolyte interface. In a typical Nyquist plot, which includes a semicircle region lying on the axis followed by a straight line, the semicircle region of the plot observed at higher frequencies corresponds to the electron transfer-limited process, whereas the linear part at the lower frequencies range represents the diffusionally limited electrochemical process.[24]

Figure 6 shows the Nyquist plot of naked BDD electrodes measured at the different DC potentials. The reason we only apply the negative DC potential here is because both the impedance modulus and the phase angles do not show any changes at positive potentials (up to +1.0 V, open- circuit potential vs Ag/AgCl). The application of a negative DC potential is also appropriate for DNA-modified BDD electrodes to prevent the oxidation of the oligonucleotides. As shown in Figure 6a, at sufficiently negative potentials of −1.0 and −0.6 V, the Nyquist plot is characterized by semicircles, indicating that the charge-transfer process at the naked BDD electrode surface is limited by electron-transfer kinetics. With the increase of the potential, the charge-transfer process switches from kinetic control to diffusion control in the Nyquist plot. The "complex plane" impedance curve reveals a deviation form the semicircle toward a limiting real impedance behavior.

Upon surface modification by PANI/PAA polymer, the impedance modulus experienced a substantial increase for the BDD electrodes. As shown in Figure 6b, at a bias potential −0.8 V, the radius of semicircle in the Nyquist plot of PANI/PAA-modified BDD electrode/electrolyte interface is much larger than that of naked BDD electrodes, which means that the charge-transfer resistance has increased significantly after electropolymerization. This result can be explained by the electrochemical properties of polyaniline. It is known that the conductivity of polyaniline is dependent on its redox states.[20] When polyaniline is fully reduced at negative potential, its conductivity becomes lower. The self-dopant cations inserted during electropolymerization are expelled into the solution phase, and the polymer is left in its neutral, less conductive state.[25]

Besides the impedance modulus change, we observed a change in the phase angle after the surface modification of BDD electrodes by the PANI/PAA polymer. Figure 6c shows the plot of phase angle versus frequency for the naked BDD electrodes and the PANI/PAA-modified BDD electrodes. A peak at ∼20−600 Hz is seen on the polymer-modified BDD. The presence of this peak indicates that an additional capacitive element is produced after BDD surface modification by the PANI/PAA copolymer film. In a previous study, Kondo et al. observed the appearance of similar peaks on anodically treated BDD electrodes[26] and attributed these to the presence of OH and C═O functional groups on the diamond surface.

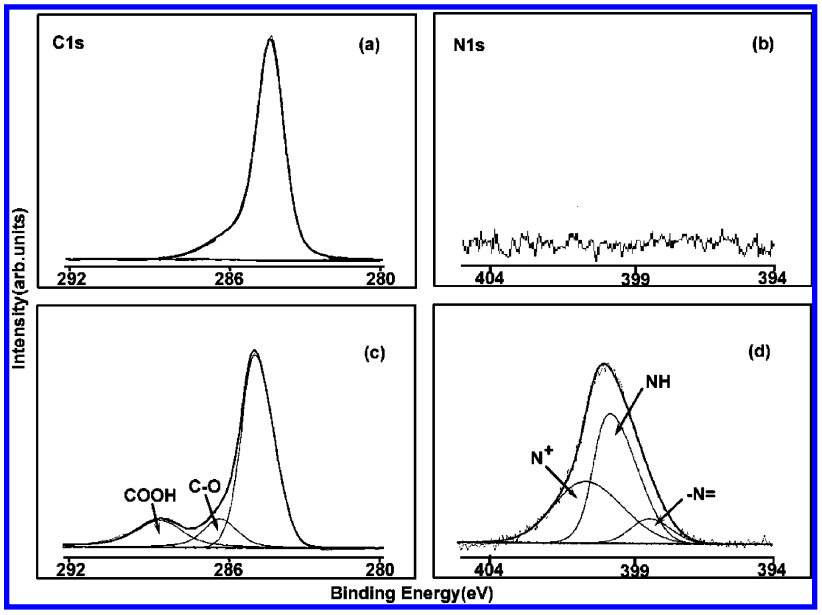

Figure 3. C1s and N1s core-level spectra of naked BDD (a and b) and PANI/PAA polymer composite film-modified BDD (c and d).

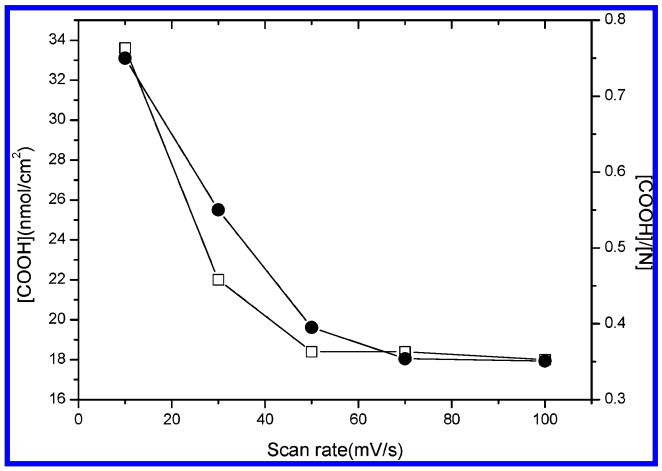

Figure 4. COOH group density quantified using TBO method and the composition of PANI/PAA polymer composite films generated using different scan rates.

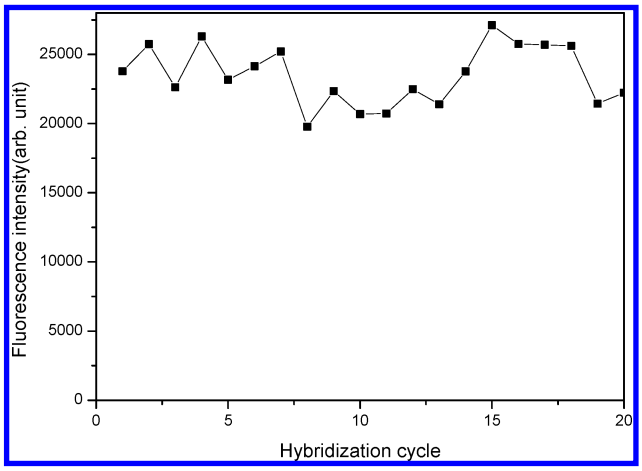

Figure 5. Fluorescence intensity of DNA probes-immobilized PANI/PAA-modified BDD electrodes surface after repeated hybridization to fully complementary FITC labeled DNA targets (1 μM in 2×SSC hybridization buffer).

After immobilization of the DNA probes on the polymer-modified BDD, impedance measurements were carried out under the same conditions as before. The questions we ask is: how does the immobilization of DNA probe on polymer-modified diamond change the impedance characteristics? After the hybridization of target DNA to the probe, what further changes can we see? Our results show that the process can be followed sensitively by impedimetric sensing at each stage. Figure 7a shows the Nyquist plot of probe-immobilized BDD electrodes measured at different potential value (open-circuit potential vs Ag/AgCl) in PBS pH 7.4 buffer. The potential dependence of the impedance, a characteristic of semiconductor behavior, is clearly seen at the high-frequency range (f > 10 kHz), a region dominated by the space charge region of diamond.

Following the immobilization of the probe DNA on the polymer-modified BDD electrode, the Nyquist plot in Figure 7b shows an increase in the diameter of the semicircle. The Bode plot in Figure 7c also shows an impedance increase, suggesting that the presence of single-stranded DNA increases the electron-transfer resistance on the surface.

Hybridization-Induced Impedance Changes and Flat-Band Potential Measurements. Figure 8 shows the Bode plot and Nyquist plot of DNA immobilized PANI/PAA-modified BDD electrode, before and after exposure to fully complementary target DNA (▲) and target DNA with one-base mismatch (○). At the frequency range between 10 and 100 Hz, a noticeable decrease of the impedance modulus from 13 to 6 kΩ appears in the Bode plot (Figure 8a) after hybridization with complimentary DNA. The decrease in impedance in the Bode plot after hybridization is paralleled by a decrease in electron-transfer resistance in the Nyquist plot shown in Figure 8b. The effect of DNA hybridization, which reduces the electron-transfer resistance on the electrode, clearly manifests as a much smaller diameter of the semicircle in the Nyquist plot after DNA hybridization. It is well known that double-stranded DNA is more conductive than single-stranded DNA. Previously it has been reported that molecular scaffolds due to alkyl chains type coupling are not sensitive to changes in surface conductivity arising from DNA hybridization due to the overall high resistance of the former, so the detection of conductivity changes at low frequency here (0.1−10 Hz) is due perhaps to the less resistive nature of the PANI/PAA polymer scaffold following DNA hybridization.[13]

The selectivity of DNA hybridization could be judged by hybridization with the target DNA that has one-base mismatch

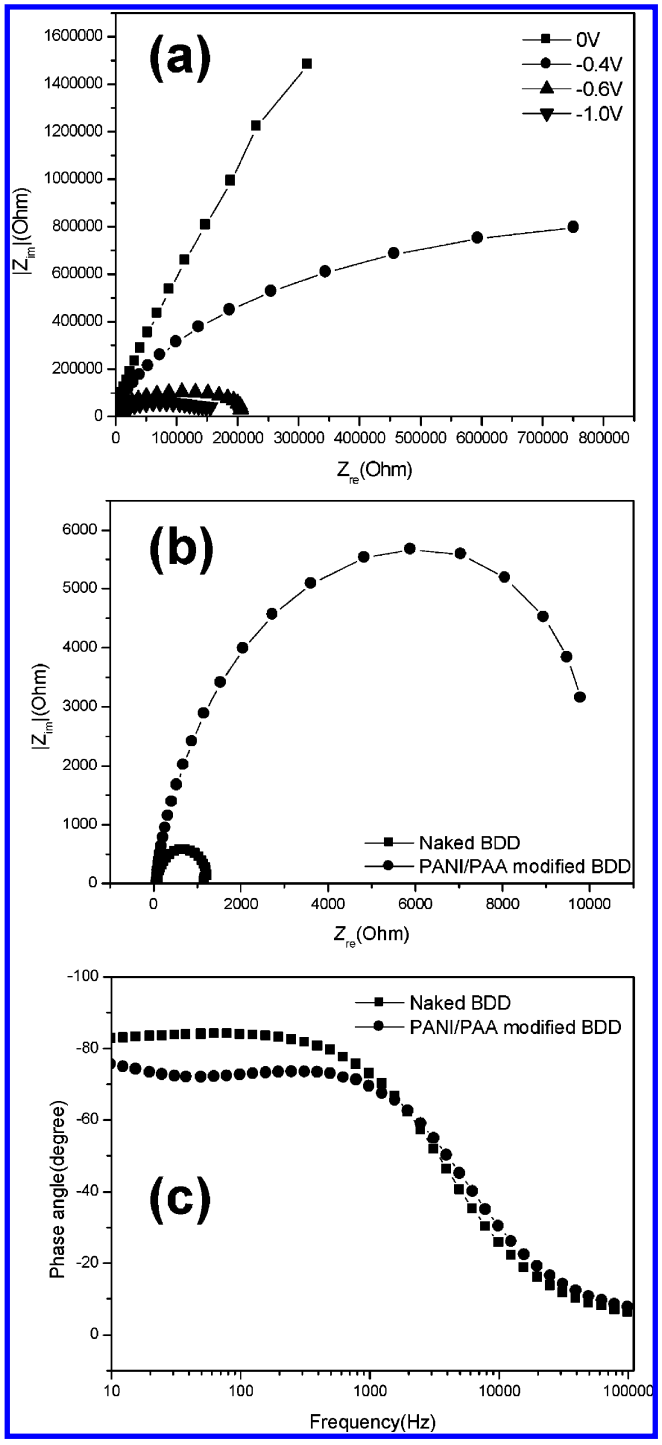

Figure 6. (a) Nyquist plot of naked BDD electrodes measured at different open-circuit potentials. (b) Nyquist plot of naked BDD and PANI/PAA-modified BDD electrodes measured at −0.8 V. (c) Bode plot of naked BDD and PANI/PAA-modified measured at −0.8 V (open-circuit potential vs Ag/AgCl).

to the surface-bound DNA probes. There is only about 20% maximum difference in the magnitude of the changes observed for fully complimentary and one-base mismatch hybridization. The impedance decrease is highlighted in the Bode plot in Figure 8a. When the targets with noncomplementary sequence were used, the impedance decrease was not observed. The changes observed at lower frequency regions in our polymer-modified BDD agree with previous study of antigen−antibody binding using the conductive polymer as the immobilization scaffold.[24] The frequency dependence of this impedance decrease differs from those reported earlier in studies of DNA hybridization

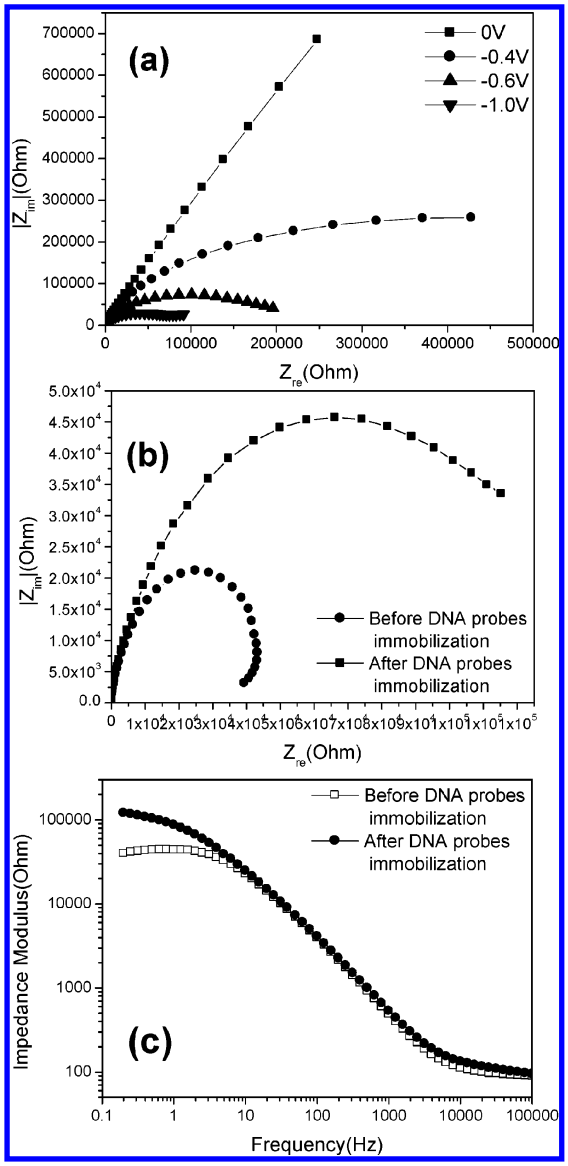

Figure 7. (a) Nyquist plot of DNA probes-immobilized PANI/PAA-modified BDD measured at the different open-circuit potentials. (b) Nyquist plot of PANI/PAA-modified BDD before and after DNA probes immobilization, measured at −0.8 V open-circuit potential vs Ag/AgCl. (c). Bode plot of PANI/PAA-modified BDD electrode before and after DNA probe immobilization, measured at −0.8 V open-circuit potential vs Ag/AgCl.

using multiwall carbon nanotubes or undoped diamond,[11,13] where the largest impedance decrease was observed at comparatively higher frequency range ($>10^4$ Hz). Therefore, our results suggest that the use of the polymer scaffold to entrap DNA allows impedimetric measurement to be measured at a lower frequency on BDD electrodes as compared to surface modification methods where DNA are coupled via short-chain hydrocarbon linkers.

To evaluate the reusability of the DNA sensing system here, the DNA-probe immobilized BDD electrode that had been hybridized with their complementary DNA targets was denatured by immersion in 0.05 M NaOH for 5 min. This treatment stripped away the target DNA that was held by weak hydrogen bonding. The denatured sensor was then subjected to a second cycle of hybridization, and the impedance measurement was conducted again. As shown in Figure 8b, after the denaturing of the DNA double-helix (curve ▽), the impedance modulus almost recovered to its original value (curve ■). Upon further

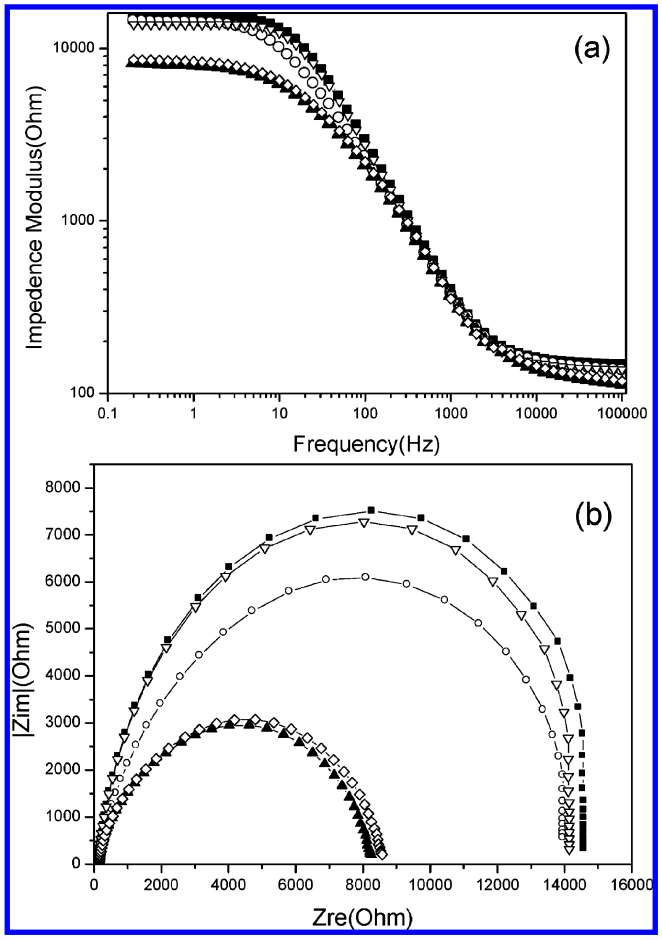

Figure 8. Impedance (a) Bode plot and (b) Nyquist plot of DNA probe-immobilized, PANI/PAA-modified BDD before (■) and after hybridization to fully complementary target (▲) or one base mismatch target (○), and after denature (▽) and renature (◇) with the fully complementary target, measured at −1.0 V open circuit potential vs Ag/AgCl.

hybridization (curve ◇), a similar decrease in impedance was observed. This indicates that the system is chemically robust, and the DNA probe remains covalently bound on the polymer matrix upon dehybridization.

Data Fitting and Electrical Response of DNA-Modified BDD Electrode Surfaces. To model the electrode/electrolyte interface based on equivalent circuit elements,[24] the BDD electrodes/electrolyte interface is divided into three physical regions, the bulk electrolyte solution, the molecular layer (including the DNA and the polymer composite thin film) and its associated double-layer, as well as the space-charge layer in the BDD electrode. The equivalent circuit model described has also been used by Yang et al.[13] for DNA-modified diamond. A schematic of the equivalent circuit elements is shown in Figure 9a, where the respective components correspond to (i) R_s, the ohmic resistance of the electrolyte solution; (ii) a parallel combination of resistor R_1 and capacitor C_1, reflecting the properties of the molecular layer and the double layer; and (iii) R_2 and constant phase element (CPE $= A^{-1}(j\omega)^{-n}$, where A and n are nonintegral, adjustable parameters, and values of $n < 1$ are attributed to surface roughness), which describe the impedance of the space charge region of the BDD electrode.

Figure 9b shows how the respective components Z_{re}, Z_{im}, and modulus Z change with frequency. Figure 9c shows one set of experimental data and its corresponding fitting data based on the circuit model for the DNA probe-immobilized BDD electrode before and after hybridization. The real and imaginary parts of the impedance were fitted simultaneously over the

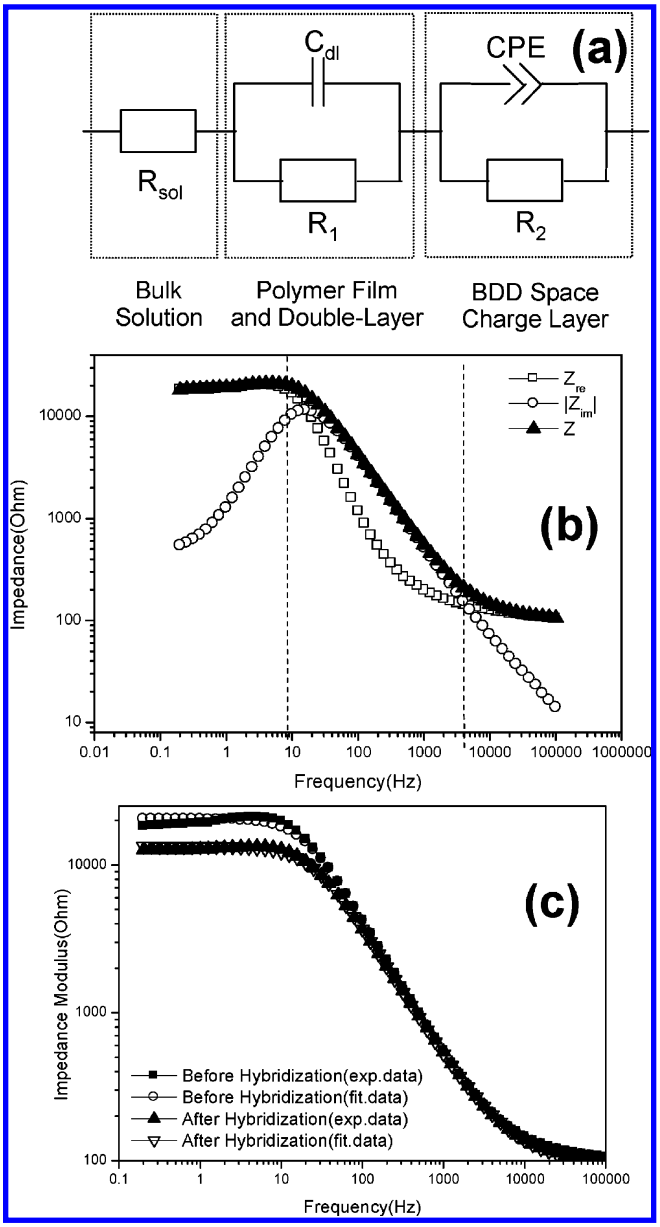

Figure 9. (a) The equivalent circuit model used for experimental data fitting. (b) Impedance real part Z_{re}, imaginary part Z_{im}, and modulus Z versus frequency change measured at −0.8 V. (c) Data fitting result of Bode plot before and after hybridization in the equivalent circuit model.

frequency range from 0.1 Hz to 1 MHz by the same set of parameters. A low χ^2 (0.02) and the applicability of the fitting to the other data indicate the validity of the equivalent circuit model we employed here. Table 1 gives the parameters fitted for DNA probe-immobilized BDD electrode before and after hybridization to complementary DNA targets, and DNA targets with one base mismatch. It is noteworthy that the capacitance (C_{dl}) of the polymer/double layer in the target-hybridized DNA is the highest at 42 μF, as compared to the probe-immobilized BDD electrode before hybridization, that is, 1.59 μF. This means that the presence of the double-stranded helix generates more charges on the electrolyte−electrode interface. From Table 1, it seems that DNA hybridization induces more significant charge redistribution within the double layer/polymer interface than in the diamond itself. The increase in capacitance and the decrease in R1 indicate that there is an increased density of ionic charges at the interface after DNA hybridization. Yang had also reported similar changes in the electrical properties of the molecular layers after hybridization.[13] The difference in this case is that

TABLE 1: Results of Fitting Parameters to the Equivalent Circuit Model, CPE = $A^{-1}(j\omega)^{-n}$, Where *A* and *n* Are Nonintegral, Adjustable Parameters, and Values of $n < 1$ Are Attributed to Surface Roughness

	R_{sol} (Ω)	C_{dl} (μF)	R_1 (kΩ)	R_2 (MΩ)	A, 10^{-5}	n
probe	163.4 ± 1.8	1.59 ± 0.15	101.8 ± 1.2	1.57 ± 0.48	2.61 ± 0.21	0.88 ± 0.01
hybridized to target	137.0 ± 1.6	42.34 ± 0.56	70.94 ± 1.04	1.21 ± 0.23	3.01 ± 0.20	0.86 ± 0.02
mismatch	148.8 ± 1.5	9.64 ± 0.22	92.31 ± 2.60	1.43 ± 0.54	1.73 ± 0.13	0.86 ± 0.01

the decrease in impedance can be clearly observed at frequencies between 10 and 100 Hz in Figure 8a, a region where circuit elements such as R_1, double layer capacitor, and CPE (space charge layer) play an equal role in the overall impedance. In Yang's work[13] involving alkyl-coupled DNA, the difference in impedance can only be detected at frequencies >10 kHz, a region where the impedance is dominated by CPE.[13] We suggest that the hybridization of DNA in the polymer scaffold decreases the impedance of the polymer significantly, resulting in dramatic changes in R_1 and C_{dl}, which can be detected at a frequency range of 10−100 Hz.

Mott−Schottky analysis is a discrete step AC voltammogram. In the Mott−Schottky analysis, the electrochemical cell impedance is measured over a range of DC offset voltages using a single test frequency. Its resistance and capacitance (assuming a simple series RC model) are plotted in real time as a function of DC voltage. This analysis is commonly used for semiconductor and film formation studies. In this study, we use the Mott−Schottky analysis to derive insights into the interfacial electrical properties of the modified BDD influenced by DNA hybridization. The Mott−Schottky equation can be used to analyze the data.

$$\frac{1}{C^2} = \frac{2}{e\epsilon\epsilon_0 N_d}\left(E - E_{FB} - \frac{kT}{e}\right)$$

where C is the effective capacitance, ϵ is the dielectric constant of the semiconductor, ϵ_0 is the permittivity of free space, e is the electron charge, N_d is the number density of donors, E is the electrode potential, E_{FB} is the flat-band potential, k is Boltzmann's constant, and T is the temperature.

Figure 10a shows the plots of capacitance ($1/C^2$) as a function of potential (V) for DNA probe-immobilized BDD electrodes, and DNA probe-immobilized BDD electrodes after exposure to DNA target, measured at 1000 Hz. The plot of $1/C^2$ versus V has the characteristic shape expected of a p-type semiconductor.[13,28] The observed capacitance behavior of the DNA−polymer−diamond interface in this work is quite similar to the report by Yang and co-workers,[13] which describes a DNA sensor based on the covalent linking of DNA molecules to a nanocrystalline diamond surface. Yang suggested that the resulting DNA-containing diamond surface has a sufficiently low density of surface states so that the energy of the valence and conduction bands can be altered by applying an external potential. From Figure 10, we can observe that the capacitance of the hybridized BDD surface is larger than that of the unhybridized surface over the entire capacitance range. This agrees well with the results of the equivalent circuit modeling discussed earlier; the double layer capacitance was found to increase significantly in Table 1 for the hybridized surface.

Because $1/C^2$ is linear over the potential range between −0.2 and 0 V as shown in Figure 10a, the flat-band potential can be obtained by extrapolating the linear range of $1/C^2$ to zero and using $kT/e = 26.1$ mV. In our measurement, the flat-band potential is 0.80 V for DNA probe-immobilized, PANI/PAA-modified BDD. This corresponds to downward band bending, that is, formation of a depletion layer at the diamond interface.

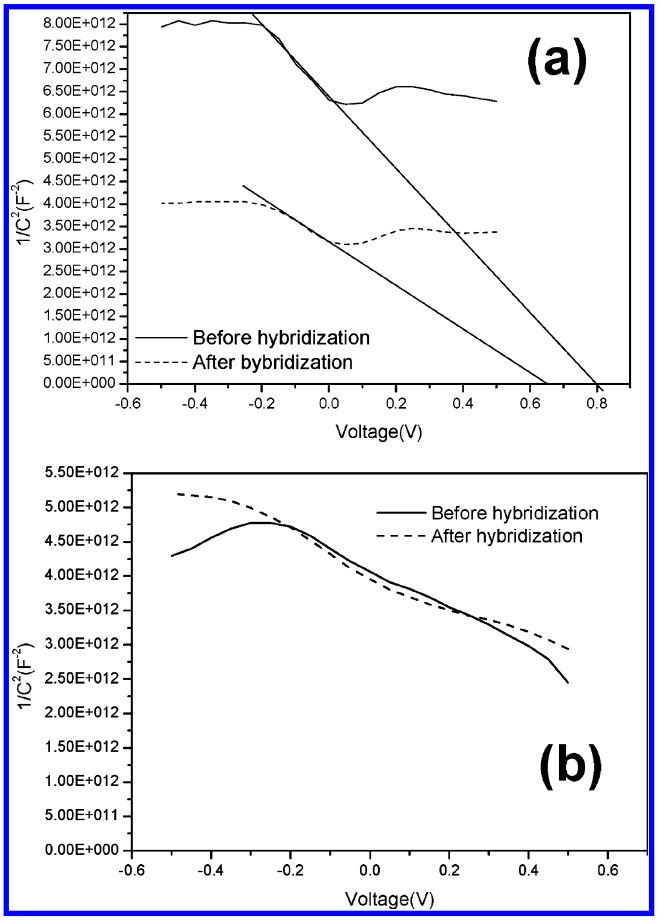

Figure 10. Mott−Schottky analysis of (a) DNA probe-immobilized, PANI/PAA-modified BDD electrodes and (b) DNA probe-immobilized, PANI/PAA-modified gold electrodes, before and after hybridization in PBS buffer (pH 7.4), measured at 1000 Hz.

This value shifts to around 0.65 V when the sample was hybridized to complementary targets. The Mott−Schottky analysis therefore indicates the hybridization to target DNA shifts the flat-band potential in the negative direction, similar to what has been reported by Yang et al.[13] on DNA-modified nanocrystalline diamond. A negative shift of the flat band potential suggests a reduction in the magnitude of downward band bending, which will result a decrease in interfacial resistance. This result is consistent with the reduction in impedance observed in the Nyquist and Bode plots in Figures 8 and 9. Binding of negatively charged DNA molecules on the BDD surface can alter the electrical response of the semiconducting diamond by inducing a "field effect", with commensurate changes in the resistance and capacitance of the space-charge region. Control experiments carried out on gold surfaces modified with PANI/PAA and immobilized with DNA, as shown in Figure 10b, do not show capacitance-voltage dependence at 1 kHz, in agreement with the expectation that a field effect is not present on metallic substrate. Our control experiments on PANI/PAA-modified gold also do not show significant decrease in the frequency region between 10 and 100 Hz in the Bode plot following DNA hybridization. This

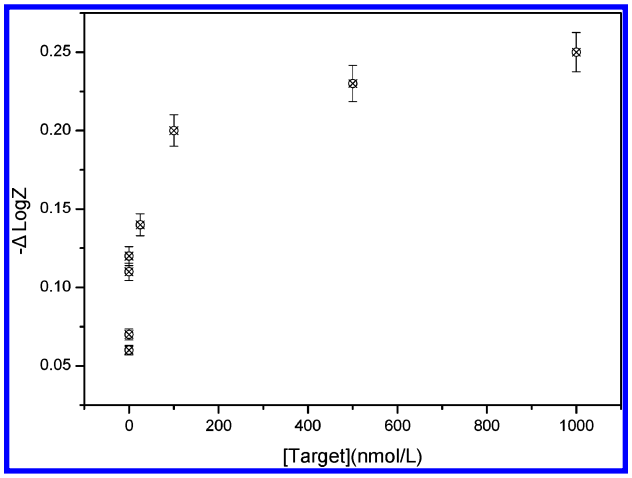

Figure 11. Difference of logarithmic impedance values obtained before and after hybridization to the complementary DNA target at different concentrations.

suggests that the enhanced detection here for DNA hybridization from 10 to 1000 Hz is due to the combined effect of capacitative changes in the molecular double layer (polymer−DNA) as well as the diamond space charge layer.

DNA Hybridization Analytical Performance. To assay the sensitivity of our DNA probe-immobilized, PANI/PAA-modified BDD electrode, the impedance changes during hybridization to the fully complementary target at different concentrations were measured. In these experiments, a concentration of 2 μM was used for the DNA probe-immobilization to saturate the binding sites of the modified BDD surface. Figure 11 plots the decrease of logarithmic impedance values, $\Delta \log Z$, as a function of different target DNA concentrations. The linearity range is from 2.0×10^{-7} to 5.0×10^{-8} M. The regression equation is $-\Delta \log Z = 8.772 \times 10^{-4}x + 0.1134$ (x is the concentration of target DNA, $\times 10^{-9}$mol/L), and the regression coefficient (r^2) of the linear curve was 0.9958. The detection limit in our case was 2×10^{-8} M using 3σ (σ is the standard deviation of blank buffer, $n = 11$). This detection limit is comparable with that of impedimetric assay of DNA hybridization using multiwall carbon nanotubes.[11] This detection limit is also comparable with that of the surface plasmon resonance spectroscopy method[29] and the quartz crystal microbalance method.[30]

4. Conclusion

A DNA sensor based on PANI/PAA-modified BDD has been fabricated. Electrochemical impedance spectroscopy has been used for the characterization of the copolymer-modified, DNA probe-immobilized BDD before and after hybridization reactions. The frequency-dependent changes in impedance of this DNA/PANI/PAA-modified BDD sensor when exposed to DNA targets show that the DNA sensor exhibits good selectivity with no nonspecific interaction. Besides acting as a scaffold for the entrapment of the nucleic acids, the copolymer-modified diamond shows enhanced sensing for DNA hybridization at low frequency, that is, 10−1000 Hz. The impedimetric sensing attained at low frequency has contributions from two sources: (1) changes in the conductivity of the polymer−DNA molecular layer following DNA hybridization. Circuit modeling shows that the capacitance as well as resistance of the polymer double layer change significantly with DNA hybridization, resulting in a visible decrease in impedance in the Bode plot at 10−100 Hz. (2) In addition, the impedance of the diamond is also found to decrease. Analysis of flat-band potentials in Mott−Schottky plots suggests that this is due to a reduction in the magnitude of downward band bending in diamond, detectable at 1 kHz. The detection limit of DNA hybridization analysis by this label-free impedance measurement is determined to be 2.0×10^{-8} M.

Acknowledgment. K. P. Loh wishes to acknowledge the financial support of NUS academic grant "Bionsensors on covalently functionalized diamond and carbon nanotube electrodes, R-143-000-192-112". H.G. thanks IMRE for the support of a graduate scholarship.

References and Notes

(1) Berggren, C.; Bjarnanson, B.; Johnsson, G. *Electroanalysis* **2001**, *13*, 173.
(2) Feng, C. D.; Ming, Y. D.; Hesketh, P. J.; Gendel, S. M.; Stetter, J. R. *Sens. Actuators, B* **1996**, *36*, 1.
(3) Kharitonov, A. B.; Alfonta, L.; Katz, E.; Willner, I. *J. Electroanal. Chem.* **2000**, *7*, 133.
(4) Alfonta, L.; Katz, E.; Willner, I. *Anal. Chem.* **2000**, *72*, 927.
(5) Alfonta, L.; Bardea, A.; Khersonsky, O.; Katz, E.; Willner, I. *Biosens. Bioelectron.* **2001**, *16*, 675.
(6) Bardea, A.; Patolsky, F.; Dagan, A.; Willner, I. *Chem. Commun.* **1999**, *1*, 21.
(7) Patolsky, F.; Lichtenstein, A.; Willner, I. *Angew. Chem., Int. Ed.* **2000**, *39*, 940.
(8) Patolsky, F.; Lichtenstein, A.; Willner, I. *J. Am. Chem. Soc.* **2001**, *123*, 5194.
(9) Vagin, M. Y.; Karyakin, A. A.; Hianik, T. *Bioelectrochemistry* **2002**, *56*, 91.
(10) Lee, T. Y.; Shim, Y. B. *Anal. Chem.* **2001**, *73*, 5629.
(11) Cai, H.; Xu, Y.; He, P. G.; Fang, Y. Z. *Electroanalysis* **2003**, *15*, 1864.
(12) Marquette, C. A.; Lawrence, I.; Polychronakos, C.; Lawrence, M. F. *Talanta* **2002**, *56*, 763.
(13) Yang, W.; Butler, J. E.; Russell, J. N., Jr.; Hamers, R. J. *Langmuir* **2004**, *20*, 6778.
(14) Swain, G. M.; Ramesham, R. *Anal. Chem.* **1993**, *65*, 345.
(15) Martin, H. B.; Argoitia, A.; Landau, U.; Anderson, A. B.; Angus, J. C. *J. Electrochem. Soc.* **1996**, *143*, L133.
(16) Yano, T.; Tryk, D. A.; Hashimoto, K.; Fujishima, A. *J. Electrochem. Soc.* **1998**, *145*, 1870.
(17) Ivandini, T. A.; Sato, R.; Makide, Y.; Fujishima, A.; Einaga, Y. *Diamond Relat. Mater.* **2004**, *13*, 2003.
(18) Rao, T. N.; Yagi, I.; Miwa, T.; Tryk, D. A.; Fujishima, A. *Anal. Chem.* **1999**, *71*, 2506.
(19) Uchida, E.; Uyama, Y.; Ikada, Y. *Langmuir* **1993**, *9*, 1121.
(20) Kang, E. T.; Neoh, K. G.; Tan, K. L.; Uyama, Y.; Morikawa, N.; Ikada, Y. *Macromolecules* **1992**, *2*, 1959.
(21) Kang, E. T.; Neoh, K. G.; Tan, K. L. *Adv. Polym. Sci.* **1993**, *106*, 135.
(22) Snauwaert, P.; Lazzaroni, R.; Riga, J.; Verbist, J. J.; Gonbeau, D. *J. Chem. Phys.* **1990**, *92*, 2187.
(23) Sano, S.; Kato, K.; Ikada, Y. *Biomaterials* **1993**, *14*, 817.
(24) Katz, E.; Willner, I. *Electroanalysis* **2003**, *15*, 913.
(25) Sargent, A.; Loi, T.; Gal, S.; Sadik, O. A. *J. Electroanal. Chem.* **1999**, *470*, 144.
(26) Kondo, T.; Honda, K.; Donald, A. T.; Fujishima, A. *Electrochim. Acta* **2003**, *48*, 2739.
(27) Gu, H. R.; Su, X. D.; Loh, K. P. *Chem. Phys. Lett.* **2004**, *388*, 483.
(28) Fang, W.; Bin, S.; Yuan, G.; Xin, S. Z. *Biosens. Bioelectron.* **2003**, *18*, 1157.
(29) Su, X. D.; Wu, Y.-J.; Robelek, R.; Knoll, W. *Langmuir* **2005**, *21*, 348.
(30) Su, X. D.; Wu, Y.-J.; Knoll, W. *Biosens. Bioelectron.*, in press.